Transp Porous Med
https://doi.org/10.1007/s11242-018-1093-3

Guidelines for Numerically Modeling Co- and Counter-current Spontaneous Imbibition

Abdul Saboor Khan[1] · **Abdul Rafey Siddiqui**[1] · **Abdul Salam Abd**[1] · **Nayef Alyafei**[1]

Received: 12 March 2018 / Accepted: 22 May 2018

Abstract We present guidelines for accurately simulating both co- and counter-current spontaneous imbibition (SI) phenomenon in 1D systems. We first consider several cases for this study, which involve strongly water-wet, weakly water-wet and mixed-wet wettability states, to simulate co- and counter-current SI in an oil–water system. We create two separate 1D models on a numerical simulator to simulate and obtain saturation profiles for the different cases. We then match simulation results with saturation profiles obtained through the capillary dominated flow semi-analytical solution proposed by Schmid et al. (Water Resour Res 47(2), 2011, SPE J 21:2–308, 2016). The numerical study evaluates the effect of model orientation and co-ordinate system on the saturation profiles. Moreover, we perform grid sensitivity analysis to choose the optimal number of grid cells, as well as the optimal time steps for the model. We find that capturing 0.25% of core volume in each grid cell is sufficient to numerically model an SI experiment within the acceptable margin of error of 5%. Simulations are performed for 23 different cases based on the SI mode, wettability and mobility ratios. The simulation results in saturation profiles have a mean absolute percentage error from the profile obtained from the semi-analytical solution between 0.14 and 5.41% for counter-current SI for the different wettability states. For most wettability states for the co-current SI, however, we do not get a close match, indicating that the semi-analytical solution does not hold for co-current SI. The paper lists some useful guidelines for simulating SI phenomenon, such as selecting the optimum number of grid cells for the SI model and accounting for capillary backpressure, which could be extended to be applied for simulating coreflooding experiments. This paper also discusses current limitations of the semi-analytical solution. These calibration and sensitivity studies can significantly improve the accuracy of the simulation results.

Keywords Spontaneous imbibition · Capillary dominated flow · Numerical simulation · Semi-analytical solution · Wettability

✉ Nayef Alyafei
nayef.alyafei@qatar.tamu.edu

[1] Department of Petroleum Engineering, Texas A&M University at Qatar, Doha, Qatar

Published online: 01 June 2018

List of symbols

F	Capillary dominated fractional flow
F'	First derivative of F
F''	Second derivative of F
f	Buckley–Leverett fractional flow
ϕ	Porosity
C	Imbibition constant (m/$\sqrt{}$s)
D	Capillary dispersion coefficient (m^2/s)
k	Permeability (m^2)
λ_w	Water mobility (1/Pa s)
λ_o	Oil mobility (1/Pa s)
λ_t	Total mobility (1/Pa s)
dP_c/dx	Capillary pressure gradient (Pa/m)
q_w	Water flow rate (m^3/s)
q_o	Oil flow rate (m^3/s)
k_{rw}	Water relative permeability
k_{ro}	Oil relative permeability
$k_{rw\,max}$	Maximum water relative permeability
$k_{ro\,max}$	Maximum oil relative permeability
S_w	Water saturation
S_w^*	Water saturation when capillary pressure is zero
S_o	Oil saturation
S_{wi}	Initial water saturation
S_{or}	Residual oil saturation
P_c	Capillary pressure (Pa)
RF	Recovery factor
P_c	Capillary pressure (Pa)
P_{entry}	Entry capillary pressure (Pa)
P_{cb}	Capillary back pressure (Pa)
n	Wetting phase exponent
m	Non-wetting phase exponent
l	Capillary pressure exponent
A_t	Actual value
F_t	Forecast value
n_i	Total number of data points
t	Time (s)
x	Distance in the core (m)
ω	Scaling factor (m/$\sqrt{}$s)

1 Introduction

Imbibition is the phenomenon where the wetting phase enters and replaces the non-wetting phase in a porous medium (Schembre et al. 1998). This process can either be forced or spontaneous. As the name suggests, forced imbibition requires external pressure to cause the wetting phase to enter the rock (Morrow and Mason 2001). On the other hand, spontaneous imbibition is the immiscible displacement of a non-wetting phase by a wetting phase

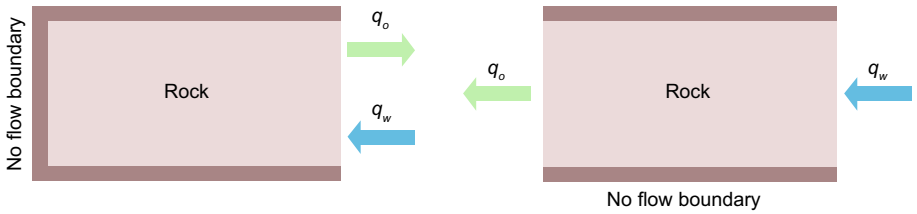

Fig. 1 Counter-current spontaneous imbibition (left) and co-current spontaneous imbibition (right) of an oil–water system in a water-wet rock. In this case, water is the wetting phase and oil is the non-wetting phase

inside porous media without any external pressure (Morrow and Mason 2001). In a reservoir, spontaneous water imbibition is the invasion of water into a porous rock to displace oil and can occur in water-wet and mixed-wet systems (Morrow and Mason 2001). In addition, spontaneous imbibition can occur in two different modes: counter-current or co-current. For counter-current spontaneous imbibition, the flow of fluids takes place at only one end; the other end is a no-flow boundary. Therefore, the wetting phase enters from one end, while the non-wetting phase exits from the same end, meaning that the flow of the two phases is in opposite directions. Conversely, co-current spontaneous imbibition is where both the ends are open and the flow of the phases is uni-directional. This means that the wetting phase enters from one end and the non-wetting phase exits from the opposite end (Unsal et al. 2007). These two modes of SI are illustrated in Fig. 1.

Spontaneous imbibition is an important recovery mechanism in fractured reservoirs, for both naturally and artificially induced fractured reservoirs. Initial production from such reservoirs is significant due to fractures, but it is followed by a relatively low production from the rock matrix. Under waterflooding in such reservoirs, the hydrocarbon production is greatly controlled by spontaneous imbibition (Morrow and Mason 2001). In addition, spontaneous imbibition has been studied as the mechanism that enables capillary trapping of CO_2. Capillary trapping occurs when water spontaneously imbibes in rocks and makes CO_2 immobile in the pore spaces. This phenomenon has significant implications for CO_2 capture and storage (CCS) (Qi et al. 2009). Having a better understanding of the rate and effectiveness of such trapping can provide an indication that a particular rock formation is appropriate for CCS.

It is known via various published literature that spontaneous imbibition is a function of interfacial tension, wettability, viscosity ratio, relative permeability and capillary pressure (Zhang et al. 1996; Mason et al. 2010; Mason and Morrow 2013). The movement of the fluid is triggered by capillary pressure, which is the difference in pressures across the interface between two phases due to surface free energy. Naturally, any system adopts an energy minimization phenomenon, in which the system favors to move to the lowest energy state (Evans and Guerrero 1979). This energy minimization process enables the displacement of the non-wetting phase by the wetting phase spontaneously, in the absence of any external pressure. Several researchers have used this information to derive analytical solutions for the spontaneous imbibition phenomenon.

1.1 Analytical Solution for Co- and Counter-current Spontaneous Imbibition

The classical Buckley and Leverett (1942) solution assumes negligible capillary pressure effects and holds true for flow with an imposed pressure difference. Therefore, we cannot use it to characterize the saturation profile for spontaneous imbibition, where the capillary pressure

has a significant involvement. Several studies have tried to come up with semi-analytical solutions to describe capillary dominated flow as a counterpart of the Buckley–Leverett solution (Yortsos and Fokas 1983; Cil and Reis 1996; Kashchiev and Firoozabadi 2003). However, most of these solutions make use of additional assumptions. McWhorter and Sunada (1990, 1992) introduce an exact integral solution that does not require assumptions of specific capillary pressure and relative permeability models. Nonetheless, it is still required to have the boundary condition for water encroachment in a specific manner. Schmid et al. (2011, 2016) portray the solution presented by McWhorter and Sunada (1990, 1992) to be a closed-form solution from which the general non-dimensional time (scaling group) can be obtained. The semi-analytical solution is developed based on the following assumptions:

1. Gravitational forces are neglected.
2. The system is homogeneous.
3. The fluids are incompressible.
4. The inlet capillary pressure is zero with no capillary backpressure (P_{cb}). Capillary backpressure is the pressure that the oil phase needs to overcome to produce oil counter-currently.
5. The traditional multi-phase Darcy law is applicable for this process.
6. The solutions are a function of the parameter $\omega = x/\sqrt{t}$ for early time, before the imbibing water front reaches the far boundaries of the sample.

Schmid and Geiger (2012, 2013) show the validity of the semi-analytical solution by scaling spontaneous imbibition experimental data with the scaling group. The results show a high level of agreement for water-wet and mixed-wet cases. In addition, the semi-analytical solution can be used to provide useful estimates of relative permeability and capillary pressure data (Alyafei et al. 2016; Khan and Alyafei 2017; Alyafei and Blunt 2018). Furthermore, the semi-analytical solution can be calculated using a very simple spreadsheet[1] available on the referenced website (Alyafei et al. 2016; Schmid et al. 2016).

The spreadsheet (see footnote 1) uses power law relationships to estimate relative permeability and capillary pressure curves, which are shown below:

$$k_{rw} = k_{rw}\max\left[\frac{S_w - S_{wi}}{1 - S_{wi} - S_{or}}\right]^n \tag{1}$$

$$k_{ro} = k_{ro}\max\left[\frac{1 - S_w - S_{or}}{1 - S_{wi} - S_{or}}\right]^m \tag{2}$$

$$P_c = P_c^{\max}\frac{\left(\frac{S_w^*}{S_{wi}}\right)^{-l} - \left(\frac{S_w}{S_{wi}}\right)^{-l}}{\left(\frac{S_w^*}{S_{wi}}\right)^{-l} - 1} \tag{3}$$

We will not discuss the derivation of the solution in this paper; the simplified explanation of the entire derivation can be found in the paper by Alyafei et al. (2016) and Schmid et al. (2016). The derivation builds upon the conservation equation for one dimensional flow of incompressible fluids:

$$\phi\frac{\partial S_w}{\partial t} + \frac{\partial q_w}{\partial x} = 0 \tag{4}$$

Using Darcy's Law, and ignoring gravitational forces and capillary back pressure, the conservation equations can be expressed as the following two equations, one for co-current flow:

[1] http://www.mfpmresearch.com/resources.html.

$$(F - f)\, F'' = -\frac{\phi}{2C^2} D \tag{5}$$

and one for counter-current flow:

$$F F'' = -\frac{\phi}{2C^2} D \tag{6}$$

where C is an imbibition constant (m/$\sqrt{}$s) to make F, which is the capillary dominated fractional flow, dimensionless, while D is the capillary dispersion coefficient (m^2/s) and is defined as:

$$D(S_w) = -\frac{k\lambda_w\lambda_o}{\lambda_t}\frac{\mathrm{d}P_c}{\mathrm{d}S_w} \tag{7}$$

Equations 5 and 6 define F that is analogous to f, the Buckley–Leverett fractional flow. The solution to the equations is presented by Schmid et al. (2011, 2016); however, it should be noted that it is only valid for the time of the imbibition where the boundary is not reached and if the amount of water imbibed scales as the square root of time. When the water front reaches the boundaries, Li and Horne (2000) and Suzanne et al. (2003) observed that the recovery rate decays exponentially. By solving the equations for F, we can obtain a water saturation profile for capillary dominated flow, comparable to the Buckley–Leverett solution with an imposed pressure.

1.2 Motivation

The purpose of this paper is to demonstrate that numerical simulation is an extremely fast and simple tool that can be used to complement saturation profiles obtained from the SI semi-analytical solution. One of the main purposes of this study is to perform a numerical analysis on SI processes using a widely available commercial simulator. The availability of the chosen simulator will help in reproducing the results easily or following the same approach to model similar processes. Although some simulators which model one-dimensional flow in porous medial will have the advantage of adapting to such imbibition processes, these simulators are not easily accessible. In this case, our approach provides details on how to model SI on a commercially available simulator, without the need of having home-written numerical simulators or specialized 1-D flow packages. This approach of choosing a commercial simulator is unique, in comparison with other numerical studies on SI like the work of Pooladi-Darvish and Firoozabadi (2000), Li and Horne (2006), and Nooruddin and Blunt (2016), who opted to code their own numerical simulators. Moreover, the numerical simulation results can be used to validate the capillary dominated flow solution proposed by Schmid et al. (2011, 2016). In addition, we describe in this paper some essential considerations and guidelines when building a numerical model for spontaneous imbibition. Obtaining a good numerical match for SI can be difficult since the volume imbibed is not a boundary condition but has to emerge from the solution. This means that more grid blocks and smaller time steps per volume are required for the corresponding Buckley–Leverett problem, as this paper will demonstrate. The recent paper by Ruth et al. (2015) models SI with 50 grid blocks, each capturing 2% of the core volume; however, our studies will show that using the SI needs to be modeled at a high number of grid blocks per volume for accuracy purposes and for the saturation profile to be closely and accurately comparable with the semi-analytical solution. This means that each grid block should capture a smaller percentage of the volume of the core.

Table 1 Details of the different cases considered in the paper. The viscosity of water and oil is 1 and 3 cP, respectively. The cores considered are each 7.66 cm in length and 2.5 cm in width

Spontaneous imbibition mode	Wetting phase	Non-wetting phase	Porosity ϕ	Permeability, k (mD)	Permeability, k (m^2)	Wettability
Counter-current	Water	Oil	0.25	1013	10^{-12}	Strongly water-wet (SWW)
Counter-current	Water	Oil	0.25	1013	10^{-12}	Weakly water-wet (WWW)
Counter-current	Water	Oil	0.25	1013	10^{-12}	Mixed wet (MW)
Co-current	Water	Oil	0.25	1013	10^{-12}	Strongly water-wet (SWW)
Co-current	Water	Oil	0.25	1013	10^{-12}	Weakly water-wet (WWW)
Co-current	Water	Oil	0.25	1013	10^{-12}	Mixed wet (MW)

2 Methodology

This section describes how the numerical model is built to simulate co- and counter-current spontaneous imbibition in cores. We consider 23 arbitrary cases with 3 wettability states, 2 SI modes, and 3–4 different mobility ratios. These cases were chosen from the cases mentioned in Blunt (2017). Table 1 shows the details of the cases, while Table 2 shows the saturation function parameters. For both the co- and counter-current cases, we are varying the mobility ratio (M), which is the mobility of the fluid that is being displaced (oil) divided by the mobility of the displacing fluid (water). In these cases, the spontaneous imbibition stops at the saturation S_w^* when the spontaneous imbibition process ends and any further recovery will require forced injection. We use the core data and saturation function curves as an input to a 1-D numerical simulation model for co- and counter-current spontaneous imbibition. Figures 2 and 3 show the saturation function curves.

2.1 Building the Simulation Grid

We use a fully implicit, three phases, and three-dimensional commercial black oil simulator to create the model. Nonetheless, our model is one dimensional and two phased. The used calculation method for the saturation and pressure is a fully implicit scheme, as it is proven to be more stable than IMPES (implicit pressure, explicit saturations) at large time steps. The fully implicit simulations are handled with care to limit any convergence errors that might rise due to the complexity of the simulated cases. We use two different approaches to model co- and counter-current spontaneous imbibition. For the counter-current model, we build the gridding in such a way that the core is represented by a number of grids of equal width. We calculate the pore volume of the core, and add an additional grid cell with a pore volume ten times that of the core attached to the end of the model. This additional cell represents

Table 2 Saturation function parameters used in the analytical solution for the cases used in this study

Parameters	SWW	WWW	MW
S_{wi}	0.1	0.1	0.1
S_{or}	0.4	0.3	0.15
S_w^*	0.6	0.6	0.5
$k_{rw\ max}$	0.1	0.2	0.5
n	2	2	8
$k_{ro\ max}$	1	1	1
m	1	1.5	2.5
P_{entry} (kPa)	200	100	100
l	0.3	0.3	0.3
$C_{counter\text{-}current}$ (m/$\sqrt{s}$)			
$M = 0.05$	4.05×10^{-4}	3.4×10^{-4}	2.72×10^{-5}
$M = 1$	3.46×10^{-4}	2.87×10^{-4}	2.64×10^{-5}
$M = 20$	1.97×10^{-4}	1.48×10^{-4}	2.48×10^{-5}
$M = 200$	8.92×10^{-5}	6.36×10^{-5}	1.76×10^{-5}
$C_{co\text{-}current}$ (m/$\sqrt{s}$)			
$M = 0.05$	4.14×10^{-4}	3.45×10^{-4}	2.69×10^{-5}
$M = 1$	4.16×10^{-4}	3.48×10^{-4}	2.69×10^{-5}
$M = 20$	4.78×10^{-4}	4.26×10^{-4}	2.69×10^{-5}

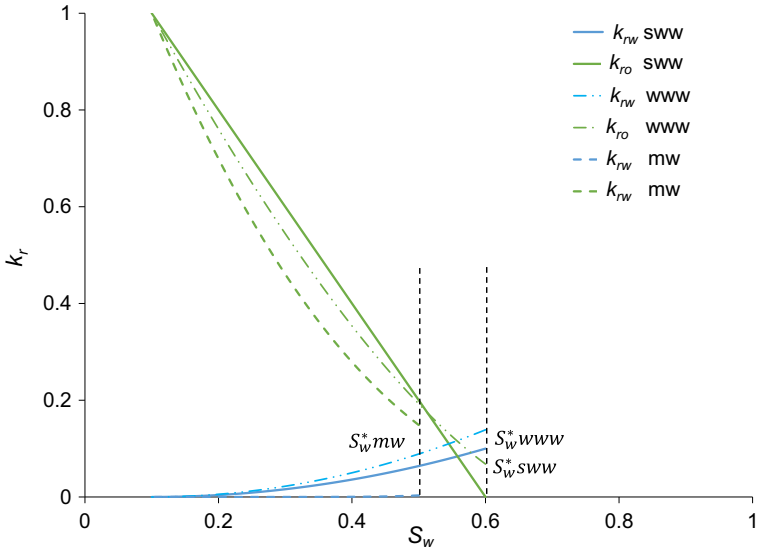

Fig. 2 Oil-water relative permeability curves for the strongly water wet, weakly water wet and mixed-wet cases. All the curves stop at their respective S_w^*

a water tank from where the spontaneous imbibition can take place. The water tank has a volume equal to ten times the pore volume of the core so that the model has sufficient water for imbibition without affecting the volume of the model significantly. For the co-current

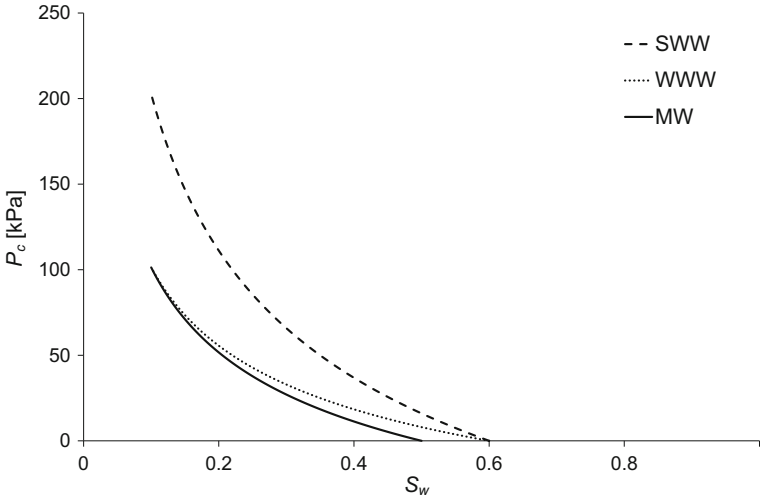

Fig. 3 Capillary pressure curves for the strongly water wet, weakly water wet and mixed-wet cases. All the curves stop at their respective S_w^*

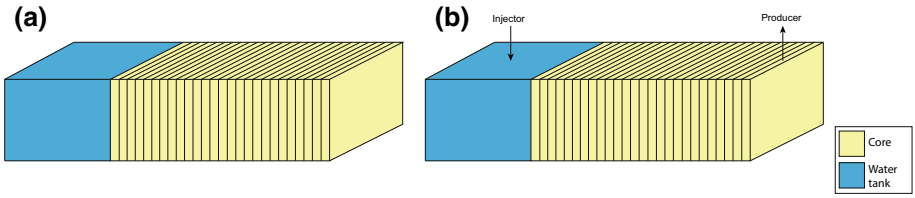

Fig. 4 Schematics showing the grid model for **a** counter-current spontaneous imbibition, and **b** co-current spontaneous imbibition of an oil–water system

model, we have the same model as the counter-current with the addition of two wells, one injector and one producer. We place the producer on one end of the model, which is the last cell representing the core. We position the injector in the cell that represents the water tank. The producer is there so that the non-wetting phase can exit the system from the other end co-currently. In addition, the injector is there to replace the wetting phase that imbibes into the cells that represent the core, thus ensuring there are no pressure imbalances in the system. The boundary conditions in this simulation are controlled using the wells. The models are illustrated in Fig. 4.

The models have two distinct regions with different saturation functions for co- and counter-current. The first region represents the core body. The properties of this region reflect the properties of the core on which we applied the semi-analytical solution. The core is assumed to be homogenous so it has constant porosity and permeability values, which are displayed in Table 1. The second region is the water tank. This region has a porosity of one, to emulate a tank, and a permeability of 10,000 mD (9.87×10^{-12} m^2) to ensure good connectivity and water flow. Moreover, we keep the oil relative permeability as one, but vary the capillary pressure to account for the effect of capillary backpressure in the system. More details will follow on the role of backpressure further in the paper.

The pressures of the wells are controlled in such a way that the pressure difference between the core and the tank is constant and equal to zero. This approach ensures that the water is

imbibing spontaneously with the absence of any external pressure from the injector well. The role of the injected water is to replace the water that has been imbibed into the core, thus preventing the backflow of oil into the water tank (uni-directional flow).

3 Model Calibration

We then calibrate the one-dimensional numerical model in order to use it for modeling spontaneous imbibition. Thereafter, we perform sensitivity studies on the numerical simulation model to capture the fluid saturation profile accurately. We observe during simulation runs that the saturation profile is sensitive to gridding orientation, co-ordinate system, temporal grid block size and capillary backpressure. We use a mixed-wet counter-current model for calibration purposes with 50 grid blocks and a time step of 120 s.

3.1 Vertical Versus Horizontal

The semi-analytical solution assumes that gravitational effects are negligible and thus can be ignored. Therefore, we create two separate models: one having a vertical orientation, and the other having a horizontal orientation. We observe from the numerical simulation that having the model in vertical and horizontal orientation to simulate SI gives saturation profiles that differ slightly. The gravitational forces in the vertical model setup cause the water-front to move slowly when compared to the horizontal model setup, which is expected since gravitational forces oppose the flow, and this can be seen in Fig. 5. We can observe in the same figure that the separation between the vertically and horizontally oriented cores increases with time. This separation between the vertical and horizontal models indicates that gravitational forces can have noticeable effects on the fluid fronts depending on the orientation of the experimental setup for SI experiments. These gravitational forces are usually ignored, but should not be as the results clearly show. One needs to take care when using the semi-analytical solution to match the experimental results; if the experiments are performed with a vertical setup, it would not be reasonably accurate to match the semi-analytical solution to it. In our case, since we are comparing semi-analytical solutions with numerical simulations, a horizontal setup is chosen to limit the effects of gravity as the semi-analytical solution ignores gravity as well.

3.2 Radial Versus Cartesian Co-ordinate Systems

In laboratory studies, spontaneous imbibition experiments are usually performed on cylindrical core samples. The numerical simulator that we use allows the model to be created in a radial co-ordinate system. However, we cannot create the radial model in a horizontal orientation. Thus, we have to use Cartesian co-ordinate system to model the core in a horizontal orientation. In order to conserve the volume of the core while converting the gridding from radial co-ordinates to Cartesian, we calculate an equivalent side dimension for the horizontal model. We do this by calculating the volume of the core. We then calculate the volume for a cuboid with the length of the core and an initial side dimension of core diameter. We match the volume of the cylinder and cuboid by varying the dimension of the side which we call equivalent side dimension. We do this to reduce any errors related to conservation of volume in the model. Therefore, for a radius of 1.25 cm in the radial system, an equivalent side dimension of approximately 2.22 cm is assigned for the Cartesian model.

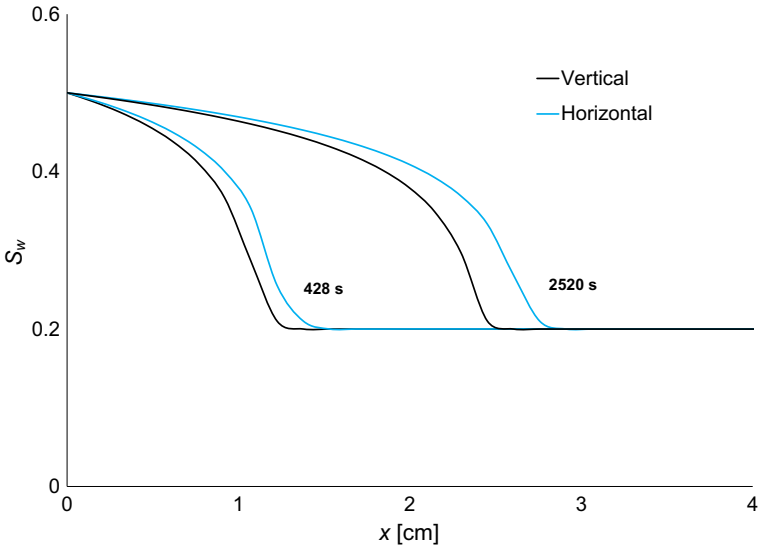

Fig. 5 Water saturation profile for vertical and horizontal orientation

To confirm if this technique works, we create a vertical model in the Cartesian co-ordinate system with the equivalent side dimension and compare it to a vertical radial core model. The saturation profiles obtained from both these models almost overlap, as shown in Fig. 6, proving that the equivalent side dimension makes the core model comparable to a radial core model. However, it should be noted that this technique might only be valid for one-dimensional model simulations and converting the co-ordinate systems in a multi-dimensional system may require additional changes. Our simulation only focuses on the 1-D aspect of the flow and, thus, a Cartesian system can be used with confidence that the results will be comparable with the flow in cylindrical cores.

3.3 Effect of Capillary Backpressure

The role of capillary backpressure in SI processes has been studied extensively by several researchers (Haugen et al. 2014; Andersen et al. 2017, 2018; Foley et al. 2017). The capillary backpressure is the pressure that the oil phase needs to overcome, in order to be produce oil counter-currently. Its significance is more evident when low oil-to-water mobility ratios (M) are encountered. This subsequently means that the recovery attributed to counter-current SI will be more substantial in low capillary backpressure scenarios. In a co-current SI setup, the face in contact with the non-wetting phase will have a P_{cb} value of 0 atm. This analysis indicates that the counter-current production can be hence enabled by assigning a value for capillary back pressure at the water tank lower or equal to the P_c value at S_w=0.

We study the effects of capillary backpressure based on a counter-current strongly water-wet SI setup. The capillary pressure of the water tank attached to the core is varied, and the results of the simulation are compared with the semi-analytical solution. From the observed plot in Fig. 7a, we notice that the quality of matching is improved when smaller P_{cb} values are used. If the P_{cb} is set to zero in the water tank, which is a practice that is recommended by Behbahani and Blunt (2005) and Behbahani et al. (2006), the maximum initial water saturation at the inlet will not be reached. The semi-analytical solution ignores the P_{cb} and

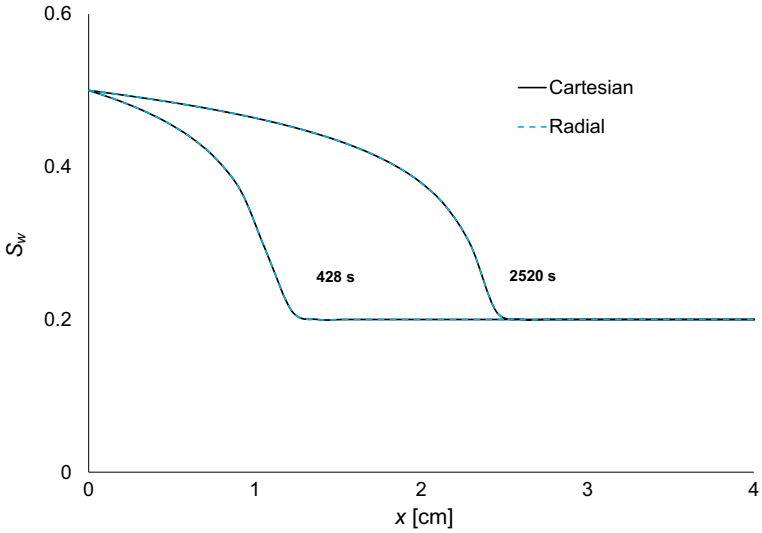

Fig. 6 Demonstration of a good match between saturation profiles obtained through radial grid model, and Cartesian grid model with an equivalent side dimension

assumes no restrictions to flow. However, the backpressure is in fact acting as a resistive force and thus trapping some of the oil in the core, and thus hindering its production through counter-current flow in the desired time. When the back pressure is reduced, the oil can move freely until the maximum initial water saturation is reached. Thus, to overcome the P_{cb}, we set the capillary pressure at the water tank to be negative. We can see that a P_{cb} value of -1 atm is required to get a match with the semi-analytical solution of an oil–water mobility ratio of $M=1$. Any value beyond this point will result in the same profile, as the maximum amount of oil that can be produced counter-currently is already achieved. The recovery plots in Fig. 7b show that the choice of the P_{cb} does not affect the total recovery of oil. The path taken by the oil might slightly differ between cases, but the maximum recovery factor (RF) is unchanged. This means that given enough time, all the recoverable oil will eventually flow out of the core even at high capillary backpressure. Based on this analysis, the P_c value in the water tank needs to be varied on a case by case basis to match the numerical profile with the semi-analytical solution. The semi-analytical solution does not consider the effects of the P_{cb} on the saturation profiles, and thus this parameter must be manipulated manually in the simulation. Furthermore, the oil and water phase pressures are plotted for the case where the numerical solution match with the semi-analytical solution for $P_c=-1$ atm. The plots can be seen in Fig. 8a–c for different simulation times. The separation between the pressure of the two phases is the maximum capillary pressure that can be observed in the system. The pressure of the water phase decreases as the water-front moves towards the outlet. The phase pressure is constant beyond the water front and, hence, the capillary pressure. If we wish to cease any production and stop the oil flow, the P_c in the water tank must be set to a value equal or greater than the capillary pressure value separating the two phases.

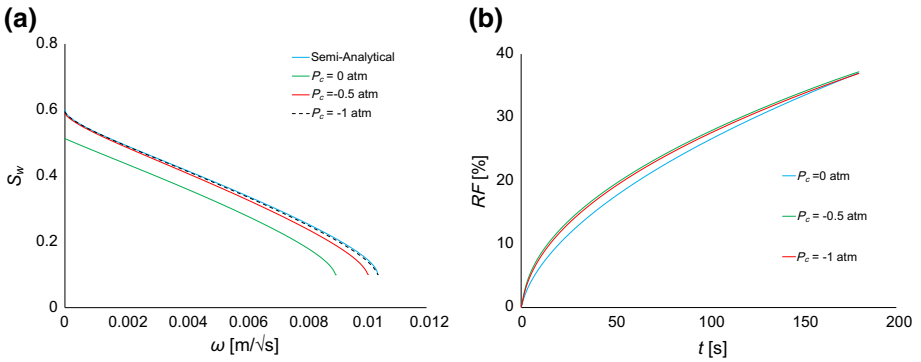

Fig. 7 **a** The water saturation profiles obtained through semi-analytical and numerical solution are compared for different capillary backpressure values. **b** The recovery factors are plotted against time for different capillary backpressures

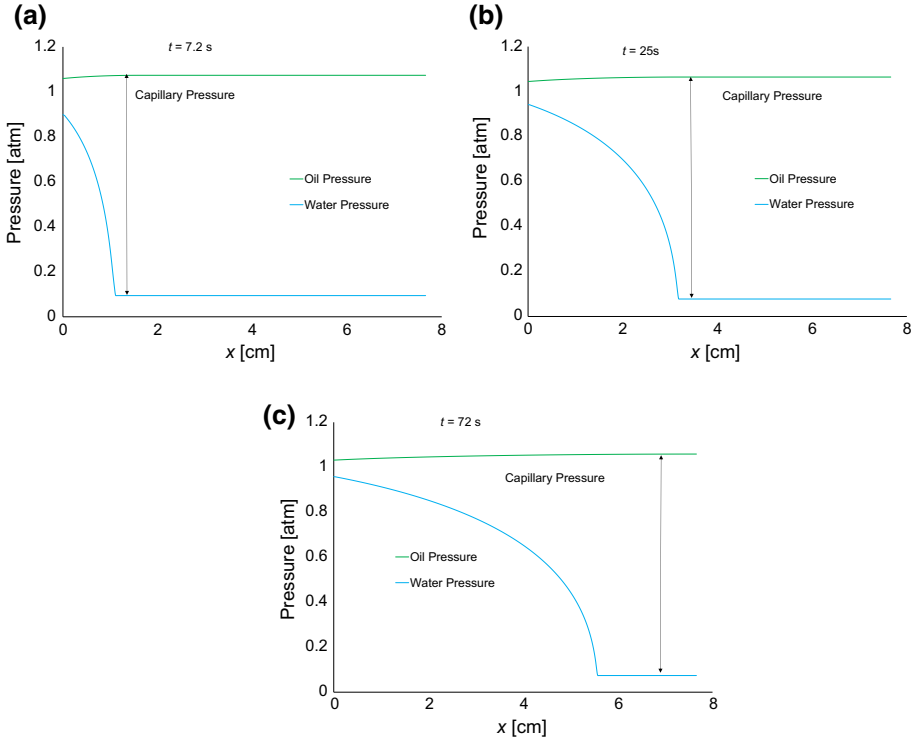

Fig. 8 Oil and water pressure throughout the core at different sample times

3.4 Uni-directional Displacement of Oil

The semi-analytical solution of Schmid et al. (2011) is developed for co-current systems based on the assumptions that all displacement of the non-wetting phase by a wetting phase occurs in a unidirectional manner. Hence, in order for the comparison of both the numerical

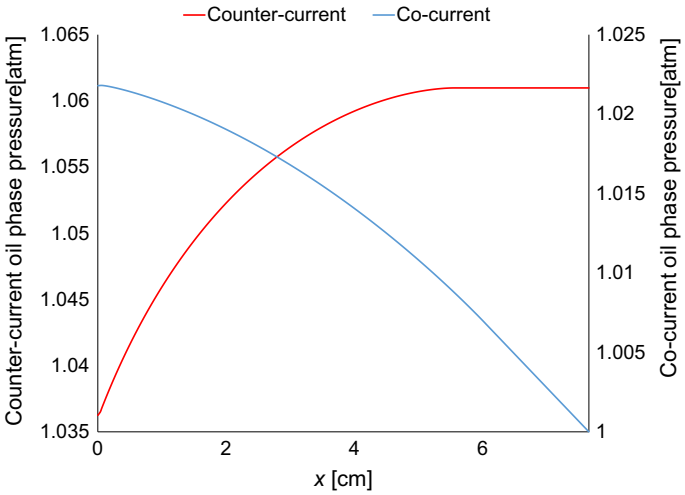

Fig. 9 Oil phase pressure throughout the core for co- and counter-current SI, which shows opposing behaviors for the two SI modes along the distance of the core

and the semi-analytical solutions to be valid, we have to ensure that the co-current flow of oil in simulation model in unidirectional, with no back-flow of oil into the water tank.

We perform numerical analysis on counter-current and co-current flow modes based on mixed-wet co- and counter-current cases. The pressure of the oil phase in both cases is plotted against the distance of the core as shown in Fig. 9. The oil pressure increases monotonically in the counter-current flow, reaching a maximum where it stays constant. The pressure cannot increase any further in this case, since a no-flow boundary is reached at the end of the sealed core. On the contrary, the co-current flow case shows that the oil pressure is decreasing while the oil flows from the inlet towards the other end and reaching the outlet. The oil pressure is thus at a minimum and has a value of 1 atm which is equivalent to the initial pressure of the system. These results agree with the analytical interpretation of the pressure behavior of the oil phase in counter-current and unidirectional co-current systems suggested by Nooruddin and Blunt (2016). The pressure gradient existing with the direction of the flow in the co-current flow indicates that it is indeed a unidirectional flow. The simulator was able to mimic this behavior by enforcing two controlled parameters; the first is the value of the P_{cb} which was set to the value of capillary pressure when the saturation of water in the system is zero, thus preventing any oil backflow. The second factor is the placement of an injector well at the water tank, which is placed to ensure that all the water that has flow into the core is being replaced efficiently. This process also ensures that there are no pressure drops occurring across the system, as the voidage replacement ratio of the fluids in the core pores is set to unity.

4 Grid Sensitivity

In this section, we evaluate the model for numerical uncertainty before obtaining results for the different cases. We run the model with a series of significantly different grid resolutions to find the grid length at which we can reach acceptable grid-convergence results. Since we

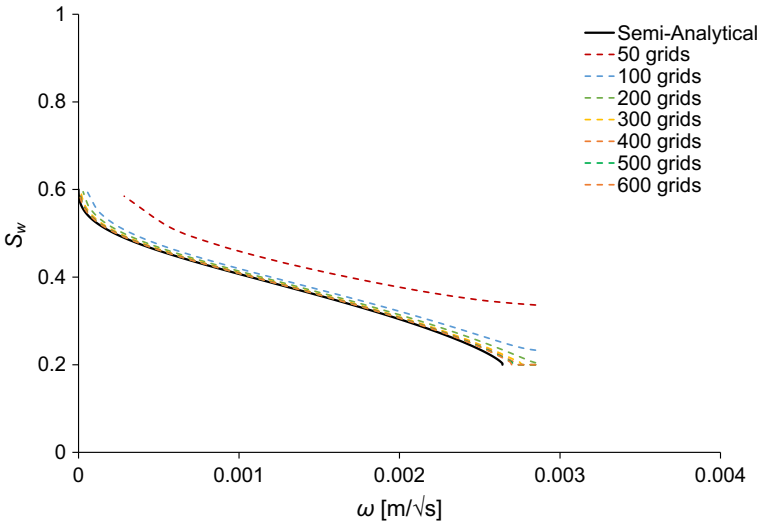

Fig. 10 Water saturation plotted against omega. The plot shows grid sensitivity study for capillary dominated flow by comparing saturation profiles obtained with various grid numbers to the semi-analytical solution

observe that the numerical simulation matches the semi-analytical solution, we can attribute the accuracy of the grid sensitivity study to how closely the simulation profile matches the semi-analytical solution result.

We run the simulation with grid sizes monotonically increasing from 50 to 1000 grids. The length of the core is constant so as the number of grid blocks increases, the percentage volume of the entire core contained by each grid block in the model decreases. The sensitivity study that we perform shows the maximum percentage volume of total core volume each grid block should contain in order to simulate a spontaneous imbibition phenomenon accurately. Moreover, the time step is varied for each grid size to ensure that the water saturation profile is smooth and continuous.

We perform sensitivity study on a modified counter-current strongly water-wet case with S_{wi}=0.2 and $M = 1$, and the results we obtained are used to decide the optimum gridding for our cases. Figure 10 shows the results obtained for the sensitivity study by scaling the water saturation profiles as $\sqrt{t}$. This ω is calculated using the following formula:

$$\omega = \frac{2CF'}{\phi} \tag{8}$$

The values of C (Table 2) and F' are obtained from the spreadsheet, and the value of ϕ is known (Table 1). This plot shows the effect of gridding from 50 to 600 grids. Beyond 600 grids, the profiles become visually indistinguishable. The black solid line shows the semi-analytical result, while the colored dashed lines represent the numerical simulation result. We can observe that we approach the semi-analytical solution as we increase the number of grids. However, we observe that the convergence is insignificant beyond 400 grid cells. Increasing the number of cells from 400 to a higher number, although resulting in further convergence with the semi-analytical solution, provides accuracy which is not required and does so at the expense of simulation time and simulation file size. An important goal of this simulation study is to achieve acceptable results while reducing the simulation time and file size.

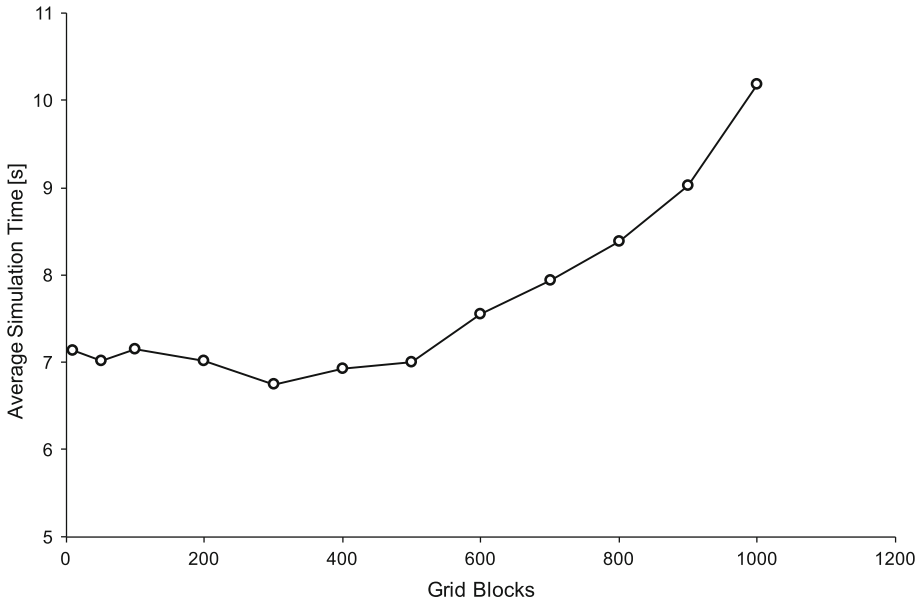

Fig. 11 Change of average runtime for numerical simulation as the number of grid blocks is varied

Furthermore, we analyze simulation time for the cases with different numbers of grid blocks. We run each case three times and calculate an average time for each case, and the obtained results are shown in Fig. 11. The workstation used in the simulation runs with a 3.60 GHz processor using a 64 GB RAM. It is evident that the simulation time remains approximately constant up to 400 grid cells. However, beyond 400 grid cells, the simulation time starts to increase significantly. Moreover, non-linear equation convergence errors also start appearing for runs with more than 400 grid cells. This error occurs when the simulator is unable to solve the material balance equations within the accuracy desired by the user even when it reduces to the minimum time step for the simulation, thus accepting the solution at that minimum time step. Figure 12 shows a linear trend between the number of grids and the simulation file size. Again, for efficiency, the goal is to limit the file size to a minimum, without compromising on accuracy. Results from both simulation time and simulation file size show that 400 grid cells are optimum to use for simulating the spontaneous imbibition process. For future cases, the number of grids might vary depending on the SI mode, since co-current SI is usually faster than counter-current SI. Also, we varied the time step for the 400 grids model, and we got a good match when a 0.72 s timestep is used. The timestep does vary from case to case and has to be optimized accordingly. In our subsequent runs, we used a variable adapting time step future, with a minimum acceptable time step of 0.05 s. The adaptive timestep makes sure that Newton's method converges to a solution within the specified CFL condition.

A more appropriate way to look at this analysis and make it independent of length is to consider percentage volume of core rather than fixed number of grids to decide on the gridding of any numerical model. Thus, we determine the maximum percentage core volume that a grid cell should contain in order to accurately model spontaneous imbibition simulation, while minimizing runtime and file size. For our sensitivity study, we find that capturing 0.25% of core volume in each grid cell is sufficient to numerically model a spontaneous

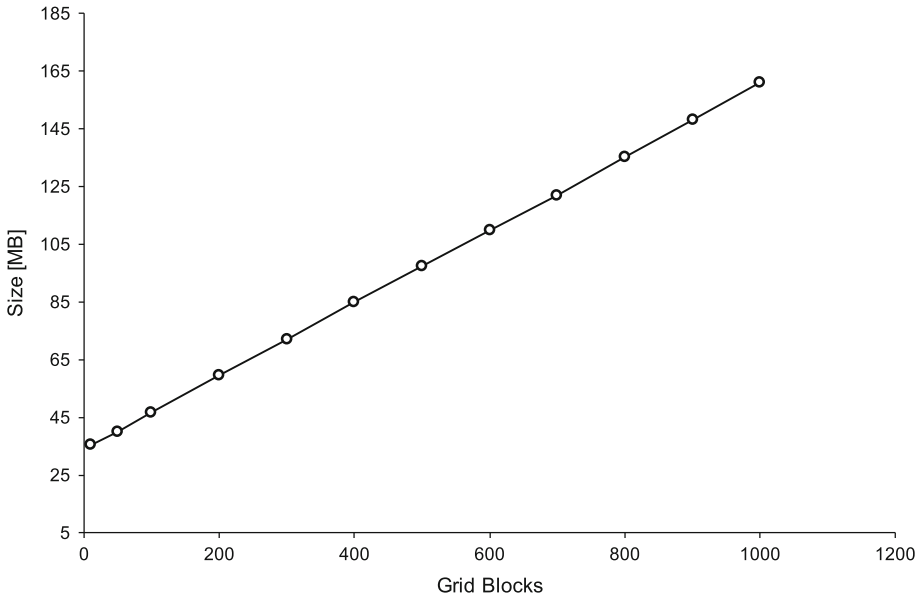

Fig. 12 Change in file size as the number of grid blocks is varied

imbibition experiment. This value gives us an acceptable error of under just under 5%, as shown in Fig. 13, when compared to the semi-analytical solution result; this value is selected because it also gives us the lowest simulation time and file size as compared to the other grid block values which also give a low error. In order to quantify the match, we perform an error analysis. For this case, we calculate the symmetric mean absolute percentage error, sMAPE (Armstrong and Forecasting 1985), the equation of which is shown below:

$$\text{sMAPE} = \frac{100}{n_i} \sum_{t=1}^{n} \frac{|F_t - A_t|}{\frac{|A_t|+|F_t|}{2}} \tag{9}$$

where A_t is the actual value, F_t is the forecast value; and n_i is the total number of data points.

To investigate the claim that this is a good measure of predicting accuracy, we vary the length of the core between realistic values, from 3 to 15 cm, to represent realistic core lengths used in experiments. The subsequent error calculations also show that having grid blocks that capture 0.25% of core volume gives us acceptable results. Subsequently, this can be taken as a rule of thumb when simulating homogenous cores for SI experiments.

The sensitivity studies are useful to evaluate spontaneous imbibition numerical models. Moreover, we also perform a grid sensitivity study on the Buckley–Leverett solution for a flow with imposed pressure difference. We do this to deduce if the same gridding principles can be used for coreflooding experiments. Once again we create a one-dimensional model, with an injector and producer positioned in the grid cells at the extreme ends of the core model. In this model, all cells represent the core and there is no water tank. We increase the number of grids monotonically, as done in the case of the spontaneous imbibition model. Figure 14 shows that, like spontaneous imbibition simulation, the Buckley–Leverett simulation also shows a grid-dependent convergence behavior with the solution, which is widely accepted. Capturing 0.25% of core volume in a grid cell is sufficient to get accurate simulation results

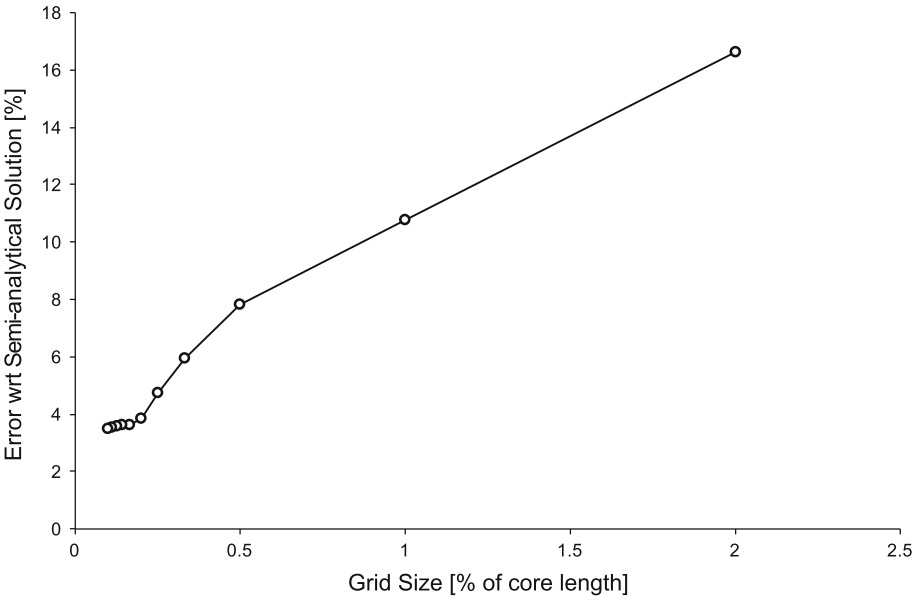

Fig. 13 Percentage error between the semi-analytical solution and the numerical simulation saturation profile as grid size is varied

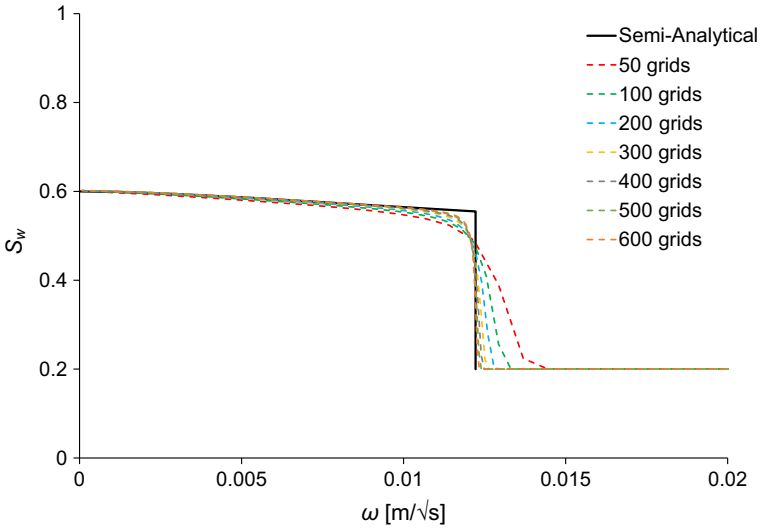

Fig. 14 The grid sensitivity study for Buckley–Leverett solution by comparing saturation profiles obtained with various grid numbers for the water-wet case. The injection rate for this case was 1.04×10^{-8} m^3/s

within the acceptable margin of error. This indicates that such a rule of thumb for gridding can be extended generally to simulating core experiments.

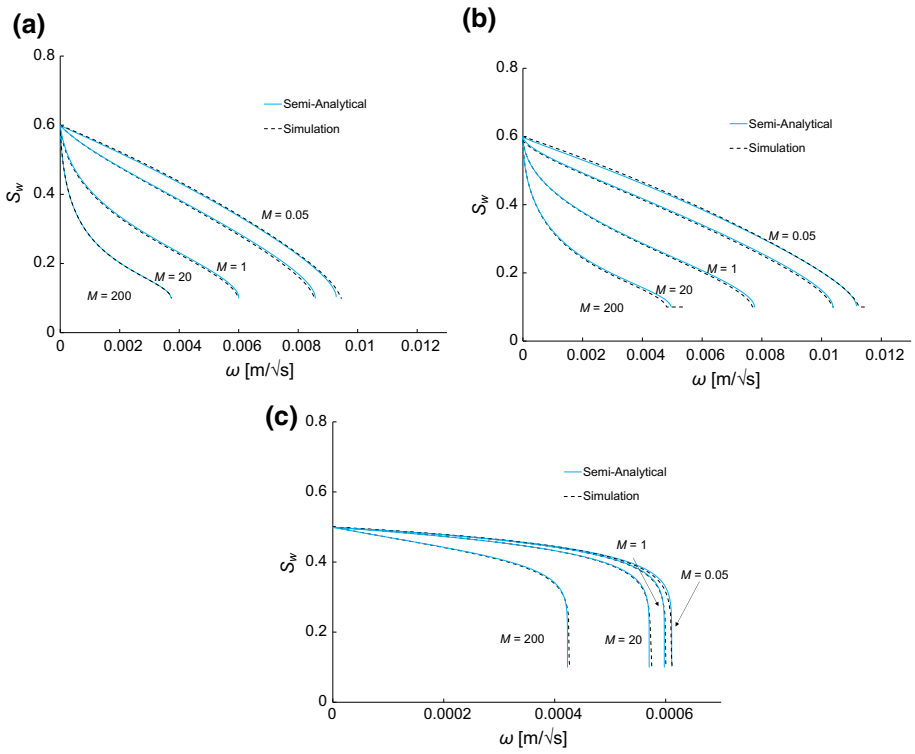

Fig. 15 A comparison between semi-analytical and numerical water saturation profiles for counter-current SI with varying mobility ratio, M, for **a** strongly water-wet case, **b** weakly water-wet case, **c** mixed-wet case

5 Semi-analytical Solution Versus Simulation

For each of the 23 cases analyzed, we run the simulation to get water saturation in each grid cell as our output from the model. We use recommendations presented in the previous sections to perform simulations on our selected cases. We divide the saturation profile by $\sqrt{t}$ for different times to check if it collapses into one curve, as proposed by Schmid et al. (2016). We then compare the collapsed curve against the semi-analytical solution to check if the two are in conformity. The results are shown in the section below, together with the semi-analytical solution result.

Figure 15 shows a comparison between the water saturation profiles from the semi-analytical solution with the saturation profile obtained from the numerical simulation. We use 400 grid blocks and a time step of 0.72 s for the cases presented. The figures present the comparison of the 3 counter-current cases, with varying mobility ratios (M). We observe that the numerical simulation saturation profile, when scaled as $\sqrt{t}$, matches the analytical solution saturation profile very closely for counter-current flow regardless of the wettability of the rock and the mobility ratio used. The time to fully saturate the rock with water is less, when the mobility ratio is low as the oil tends to move easier in the pores. The capillary pressure in the water tank is varied per case to get a match with the semi-analytical solution and diminish the effects of capillary back pressure on the results (Table 3).

Table 3 sMAPE between the analytical solution and numerical simulation result

Case	Spontaneous imbibition mode	Wettability	Mobility ratio (M)	Simulation capillary pressure (atm)	sMAPE (%)
1	Counter-current	Strongly water-wet	0.05	− 0.2	1.12
2			1	− 0.3	1.42
3			20	− 5	2.00
4			200	− 12	5.41
5		Weakly water wet	0.05	− 0.1	1.31
6			1	− 0.5	1.39
7			20	− 1.5	2.00
8			200	− 5	2.22
9		Mixed wet	0.05	0	0.14
10			1	− 0.4	0.74
11			20	− 0.5	0.65
12			200	− 0.5	0.38
13	Co-current	Strongly water wet	0.05	0	2.87
14			1	0	28.50
15			20	− 1	51.88
16			20	0	56.30
17		Weakly water wet	0.05	0	2.25
18			1	0	8.64
19			20	− 1	19.75
20			20	0	41.92
21		Mixed wet	0.05	0	1.67
22			1	0	1.67
23			20	0	1.19

However, for co-current flow, some discrepancies between the semi-analytical and the numerical solutions have been spotted at late imbibition time, where the semi-analytical solution predicts faster flow of the water in the core. In Fig. 16, a co-current mixed-wet SI process is shown. We notice that both semi-analytical and numerical solutions match for low mobility ratios less than 20. As the oil becomes more viscous, the simulation predicts a slower profile for the water front, which leads to a mismatch for the saturation at the outlet of the core. This mismatch is observed in Figs. 17 and 18 which represents a co-current weakly water-wet and strongly water-wet SI processes, respectively. In Fig. 17a, where the mobility ratio is set to 0.05, the numerical and semi-analytical profiles match closely. The degree of this match decreases as we increase the mobility ratio to 1 as seen in Fig. 17b. Moreover, the profiles in Fig. 18 show that both the numerical and semi-analytical solutions do not match for high mobility ratios either as we change the wettability of the rock to strongly water-wet. It is important to note that we use a capillary backpressure, P_{cb}, value of 0.98 atm to limit any counter-current production of oil, thus ensuring the unidirectional flow of oil. Furthermore, we increase the mobility ratio to 20 for both wettability states, and we plot the water saturation profiles shown in Fig. 19. Both cases with different wettabilities show that initial maximum water saturation at the inlet is not reached in the desired time, when the capillary pressure

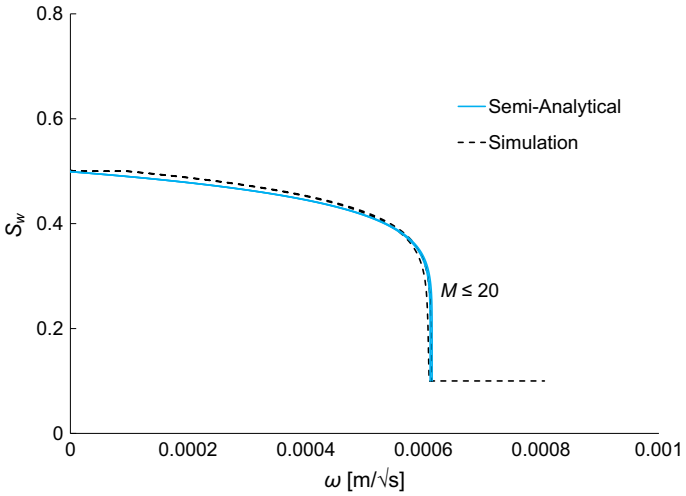

Fig. 16 A comparison between semi-analytical and numerical water saturation profiles for mixed-wet co-current SI with varying mobility ratio, M. The match is valid for all mobility ratios less than 20

in the water tank is set to 0 atm. Typically, we should set the P_c in the water tank to around 0.98 atm which corresponds to the maximum achievable capillary pressure in the core when the water saturation is zero, thus limiting any counter-current oil production. But this will only increase the mismatch in the water saturation at the inlet, rendering our simulation invalid. Hence, we try to decrease the capillary pressure in the water tank—meaning that the capillary back pressure is decreasing as well—up until we get a match to the initial maximum water saturation at a value of -1 atm. Both the wetting cases in Fig. 19a, b show that the end water saturation at the outlet can be matched with such a low P_c value. These results correspond with the conclusions of Foley et al. (2017), in which they focus on the importance of imposing the correct inlet saturation to get a match with the semi-analytical solution. In addition, the oil phase pressure plotted in Fig. 20 shows that pressure has a bell-shaped curve where it starts increasing till it reaches an inflection point where the flow of oil is zero. At that point, oil moves in different directions that corresponding to counter-current and co-current production. The pressure graphs are overlapped with the saturation profile using the same scale to detect the saturation at which the oil flow changes from counter-current to co-current. The water saturation values are found to be 0.39 and 0.32 for weakly water-wet and strongly water-wet cases, respectively. The shape of the water saturation profile obtained through the simulation when $P_c = -1$ atm is used suggests that we have a co-current production with a degree of counter-current flow, similar to what has been proved by Nooruddin and Blunt (2016).

The mismatch in co-current SI has been observed in several studies and shows that co-current imbibition for oil/water system does not scale as $\sqrt{t}$ (Nooruddin and Blunt 2016; Mason et al. 2010; Fernø et al. 2014). In this case, the proper time scaling needs to be found which will lead to a new semi-analytical solution for co-current flow.

To quantify the match, we calculate sMAPE for each case and present it in Table 3. In these calculations, each water saturation data point from the semi-analytical solution is compared with an equivalent water saturation data point from the numerical simulation, whereby the value of ω is the same. It can be seen that the error is much more significant for the co-current cases, when compared with counter-current cases. The error for the counter-current cases

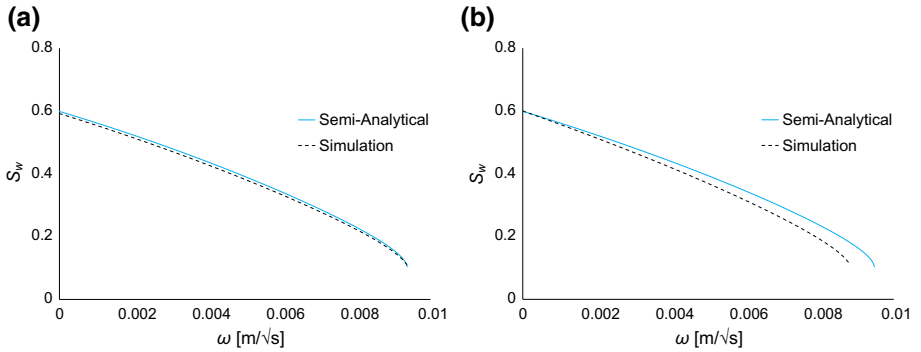

Fig. 17 A comparison between semi-analytical and numerical water saturation profiles for weakly water-wet co-current SI for **a** Mobility ratio is equal to 0.05, **b** Mobility ratio is equal to 1

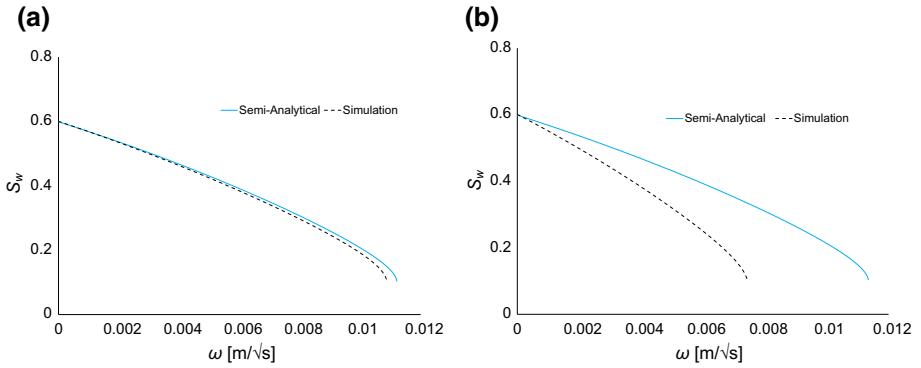

Fig. 18 A comparison between semi-analytical and numerical water saturation profiles for strongly water-wet co-current SI for **a** Mobility ratio is equal to 0.05, **b** Mobility ratio is equal to 1

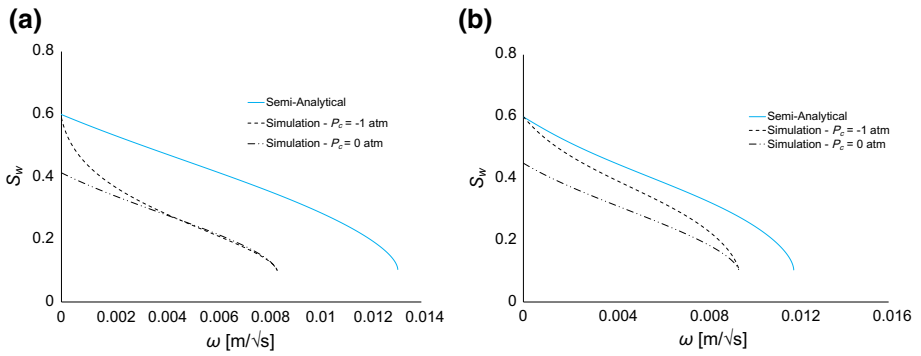

Fig. 19 A comparison between semi-analytical and numerical water saturation profiles for co-current SI with mobility ratio M = 20 for **a** strongly water-wet case, **b** weakly water-wet case

barely exceeds 5% for all the cases, whereas the error is much higher for the co-current cases with the exception of the mixed-wet cases.

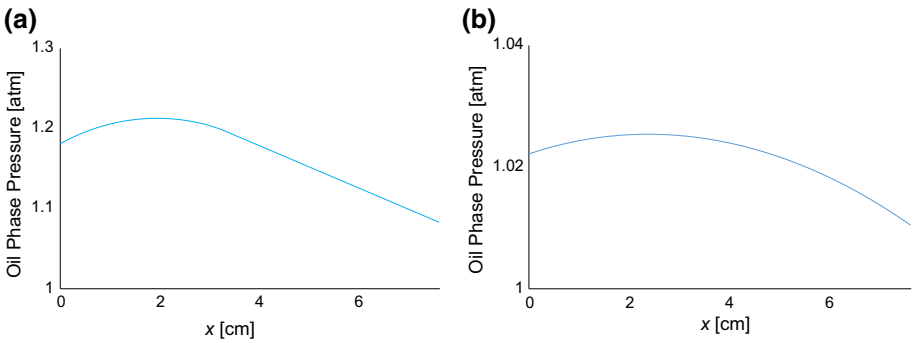

Fig. 20 The oil phase pressure is plotted against distance for co-current SI with mobility ratio M = 20 for **a** weakly water-wet case, **b** strongly water-wet case

6 Conclusions

We find that for our sensitivity study, capturing 0.25% of core volume in each grid cell is sufficient to numerically model a spontaneous imbibition experiment within the acceptable margin of error of 5% for the counter-current case. We also observe that the semi-analytical solution matches closely with the numerical simulation for all the counter-current wettability states presented in this paper and these results can be used as a way to calibrate the numerical models. However, for the co-current cases, we do not observe a close match between the semi-analytical solution and the numerical simulation for the different wettability states, with the exception of the mixed-wet case. This indicates that the current semi-analytical solution does not hold true for co-current SI and this will, therefore, require modifications to the current solution to address co-current SI.

Moreover, we lay down in this paper simple but critical guidelines that we take into consideration when forming the simulation model. We consider the effect that capillary backpressure has on the simulations, and we adjust the P_{cb} values accordingly to ensure that oil production is not hindered. In most cases, the P_{cb} values are negative so that the oil can overcome the resistive forces in the core.

The results encourage the use of numerical simulation in combination with the semi-analytical solution to provide accurate results in a very short amount of time. In addition, using the numerical model we can also check the validity of spontaneous imbibition experiments. With the different sensitivities and calibration methods discussed in this paper, our intent has been to demonstrate the impact of alignment, gridding and orientation in simulating spontaneous imbibition, which has applications in core experiments.

Acknowledgements We would like to thank Texas A&M University at Qatar for funding this project. In addition, we would like to thank Prof. Martin J. Blunt for his insightful comments and suggestions.

References

Akin, S., Schembre, J.M., Bhat, S.K., Kovscek, A.R.: Spontaneous imbibition characteristics of diatomite. J. Petrol. Sci. Eng. **25**(3), 149–165 (2000)

Alyafei, N., Al-Menhali, A., Blunt, M.J.: Experimental and analytical investigation of spontaneous imbibition in water-wet carbonates. Transp. Porous Media **115**(1), 189–207 (2016)

Alyafei, N., Blunt, M.J.: Estimation of relative permeability and capillary pressure from mass imbibition experiments. Adv. Water Resour. **115**, 88–94 (2018)

Andersen, P.Ø., Brattekås, B., Walrond, K., Aisyah, D.S., Nødland, O., Lohne, A., Haugland, H., Føyen, T.L., Fernø, M.A.: Numerical interpretation of laboratory spontaneous imbibition-incorporation of the capillary back pressure and how it affects SCAL. In: SPE Abu Dhabi International Petroleum Exhibition & Conference. Society of Petroleum Engineers (2017)

Andersen, P.Ø., Qiao, Y., Standnes, D.C., Evje, S.: Co-current spontaneous imbibition in porous media with the dynamics of viscous coupling and capillary back pressure. In: SPE Improved Oil Recovery Conference. Society of Petroleum Engineers (2018)

Armstrong, J.S., Forecasting, L.R.: From crystal ball to computer. New York ua (1985)

Behbahani, H., Blunt, M.J.: Analysis of imbibition in mixed-wet rocks using pore-scale modeling. SPE J. **10**(04), 466–474 (2005)

Behbahani, H.S., Di Donato, G., Blunt, M.J.: Simulation of counter-current imbibition in water-wet fractured reservoirs. J. Petrol. Sci. Eng. **50**(1), 21–39 (2006)

Blunt, M.J.: Multiphase flow in permeable media: a pore-scale perspective. Cambridge University Press, Cambridge (2017)

Buckley, S.E., Leverett, M.: Mechanism of fluid displacement in sands. Trans. AIME **146**(01), 107–116 (1942)

Chen, Z.X., Bodvarsson, G.S., Witherspoon, P.A.: Comment on "Exact integral solutions for two-phase flow" by David B. McWhorter and Daniel K. Sunada. Water Resour. Res. **28**(5), 1477–1478 (1992)

Cil, M., Reis, J.C.: A multi-dimensional, analytical model for counter-current water imbibition into gas-saturated matrix blocks. J. Petrol. Sci. Eng. **16**(1–3), 61–69 (1996)

Evans, C.E., Guerrero, E.T.: Theory and application of capillary pressure. In: SPWLA 20th annual logging symposium. Society of Petrophysicists and Well-Log Analysts (1979)

Fernø, M.A., Haugen, Å., Mason, G., Morrow, N.R.: Measurement of core properties using a new technique–two ends open spontaneous imbibition. In: Proceedings of Society of Core Analysts held in Avignon, France (2014)

Foley, A.Y., Nooruddin, H.A., Blunt, M.J.: The impact of capillary backpressure on spontaneous counter-current imbibition in porous media. Adv. Water Resour. **107**, 405–420 (2017)

Haugen, Å., Fernø, M.A., Mason, G., Morrow, N.R.: Capillary pressure and relative permeability estimated from a single spontaneous imbibition test. J. Petrol. Sci. Eng. **115**, 66–77 (2014)

Kashchiev, D., Firoozabadi, A.: Analytical solutions for 1D countercurrent imbibition in water-wet media. SPE J. **8**(04), 401–408 (2003)

Khan, A.S., Alyafei, N.: Investigation of an analytical solution for spontaneous imbibition to effectively estimate special core analysis SCAL properties (Russian). In: SPE Annual Caspian Technical Conference and Exhibition. Society of Petroleum Engineers (2017)

Li, K., Horne, R.N.: Characterization of spontaneous water imbibition into gas-saturated rocks. In: SPE/AAPG Western Regional Meeting. Society of Petroleum Engineers (2000)

Li, K., Horne, R.N.: Generalized scaling approach for spontaneous imbibition: an analytical model. SPE Reserv. Eval. Eng. **9**(03), 251–258 (2006)

Mason, G., Fischer, H., Morrow, N.R., Johannesen, E., Haugen, Å., Graue, A., Fernø, M.A.: Oil production by spontaneous imbibition from sandstone and chalk cylindrical cores with two ends open. Energy Fuels **24**(2), 1164–1169 (2010)

Mason, G., Morrow, N.R.: Developments in spontaneous imbibition and possibilities for future work. J. Petrol. Sci. Eng. **110**, 268–293 (2013)

McWhorter, D.B., Sunada, D.K.: Exact integral solutions for two-phase flow. Water Resour. Res. **26**(3), 399–413 (1990)

McWhorter, D.B., Sunada, D.K.: Reply [to "Comment on 'Exact integral solutions for two-phase flow' by David B. McWhorter and Daniel K. Sunada"]. Water Resour. Res. **28**(5), 1479 (1992)

Morrow, N.R., Mason, G.: Recovery of oil by spontaneous imbibition. Curr. Opin. Colloid Interface Sci. **6**(4), 321–337 (2001)

Nooruddin, H.A., Blunt, M.J.: Analytical and numerical investigations of spontaneous imbibition in porous media. Water Resour. Res. **52**(9), 7284–7310 (2016)

Pooladi-Darvish, M., Firoozabadi, A.: Cocurrent and countercurrent imbibition in a water-wet matrix block. SPE J. **5**(01), 3–11 (2000)

Qi, R., LaForce, T.C., Blunt, M.J.: Design of carbon dioxide storage in aquifers. Int. J. Greenh. Gas Control. **3**(2), 195–205 (2009)

Ruth, D.W., Mason, G., Fernø, M.A., Haugen, Å., Morrow, N.R., Arabjamaloei, R.: Numerical simulation of combined co-current/counter-current spontaneous imbibition. In: International Symposium of the Society of Core Analysts, pp. 16–21 (2015)

Schembre, J., Akin, S., Kovscek, A.R.: Spontaneous imbibition in low permeability media. Doctoral dissertation, Stanford University (1998)

Schmid, K.S., Geiger, S., Sorbie, K.S.: Semianalytical solutions for cocurrent and countercurrent imbibition and dispersion of solutes in immiscible two-phase flow. Water Resour. Res. **47**(2), W02550 (2011)
Schmid, K.S., Geiger, S.: Universal scaling of spontaneous imbibition for water-wet systems. Water Resour. Res. **48**(3), W03507 (2012)
Schmid, K.S., Geiger, S.: Universal scaling of spontaneous imbibition for arbitrary petrophysical properties: water-wet and mixed-wet states and Handy's conjecture. J. Petrol. Sci. Eng. **101**, 44–61 (2013)
Schmid, K.S., Alyafei, N., Geiger, S., Blunt, M.J.: Analytical solutions for spontaneous imbibition: fractional-flow theory and experimental analysis. SPE J. (2016). https://doi.org/10.2118/184393-PA
Suzanne, K., Hamon, G., Billiotte, J., Trocme, V.: Experimental relationships between residual gas saturation and initial gas saturation in heterogeneous sandstone reservoirs. In: SPE Annual Technical Conference and Exhibition. Society of Petroleum Engineers (2003)
Unsal, E., Mason, G., Morrow, N.R., Ruth, D.W.: Co-current and counter-current imbibition in independent tubes of non-axisymmetric geometry. J. Colloid Interface Sci. **306**(1), 105–117 (2007)
Yortsos, Y.C., Fokas, A.S.: An analytical solution for linear waterflood including the effects of capillary pressure. Soc. Petrol. Eng. J. **23**(01), 115–124 (1983)
Zhang, X., Morrow, N.R., Ma, S.: Experimental verification of a modified scaling group for spontaneous imbibition. SPE Reserv. Eng. **11**(04), 280–285 (1996)